Inelastic neutron scattering investigation of the magnetic excitations in the helimagnetic state of NiBr2

L.P. Régnault, J. Rossat-Mignod, A. Adam, D. Billerey, C. Terrier

J. Physique **43** (1982) 1283-1290 AOÛT **1982,** PAGE 1283

Classification
Physics Abstracts
75.30D

Inelastic neutron scattering investigation of the magnetic excitations in the helimagnetic state of $NiBr_2$

L. P. Régnault, J. Rossat-Mignod

Laboratoire de Diffraction Neutronique, Département de Recherche Fondamentale, Centre d'Etudes Nucléaires, 85 X, 38041 Grenoble Cedex, France

A. Adam, D. Billerey and C. Terrier

Laboratoire de Thermomagnétisme, Université de Nancy, 54037 Nancy, France

(*Reçu le 2 mars 1982, révisé le 26 avril, accepté le 29 avril 1982*)

Résumé. — Une étude du spectre d'onde de spin par diffusion inélastique des neutrons a été effectuée sur le composé $NiBr_2$ à $T = 4{,}2$ K afin de déterminer les paramètres d'échange et d'anisotropie. Ces paramètres sont nécessaires pour la compréhension de la transition hélimagnétique antiferromagnétique qui a lieu à $T_{IC} = 22{,}8$ K dont l'origine est assez inhabituelle.
Nous trouvons que la dynamique de spin dans $NiBr_2$ peut être décrite par un hamiltonien d'échange isotrope pour un spin $S = 1$ avec les constantes d'échange dans les plans $J_1 = 1{,}56$ meV, $J_2 = -0{,}018$ meV et $J_3 = -0{,}41$ meV, un faible couplage entre plans $J' = -0{,}182$ meV et une anisotropie du type XY $D = 0{,}15$ meV. Nous soulignons que pour une structure hélimagnétique les composantes de spin perpendiculaires et contenues dans le plan de base donnent lieu à des pics dans l'intensité des neutrons diffusés aux énergies $\omega(\mathbf{q})$ et $\omega(\mathbf{q} \pm \mathbf{k}_0)$ respectivement. Ces trois pics ont effectivement été observés dans les expériences sur $NiBr_2$.

Abstract. — We report on an inelastic neutron scattering study of the spin waves in $NiBr_2$ at $T = 4.2$ K, performed in order to determine the exchange and anisotropy parameters. These are needed in order to understand the unusual helimagnetic-antiferromagnetic transition which occurs at $T_{IC} = 22.8$ K. We find that the spin dynamics of $NiBr_2$ can be described by an isotropic exchange hamiltonian for $S = 1$ with in-plane exchange constants $J_1 = 1.56$ meV, $J_2 = -0.018$ meV and $J_3 = -0.41$ meV, a weak inter plane coupling $J' = -0.182$ meV, and an anisotropy of XY-type $D = 0.15$ meV. We point out that in a helimagnetically ordered phase the out-of-plane and the in-plane spin components may give rise to peaks in the neutron scattering intensity at energies $\omega(\mathbf{q})$ and $\omega(\mathbf{q} \pm \mathbf{k}_0)$, respectively. These three peaks have actually been observed in our experiments on $NiBr_2$.

1. **Introduction.** — Anhydrous nickel bromide is known to order antiferromagnetically below $T_N = 52$ K [1], with a magnetic structure similar to that of $NiCl_2$ [2] consisting of a stack of ferromagnetic (001) planes in a $(+ - + -)$ sequence. The magnetic moments are within the (001) planes. Below $T_{IC} \simeq 22.8$ K a new phase has been observed [1, 3, 4] which has been recently identified as an incommensurate phase [5, 6]. The ordering within (001) planes becomes helimagnetic whereas the coupling between planes remains antiferromagnetic. The helix propagates along a $\langle 110 \rangle$ direction with a wave vector $\mathbf{k}_0 = [0.027, 0.027, 3/2]$ at $T = 4.2$ K (Fig. 1) [6]. The small incommensurate component of the wave vector decreases with increasing temperature up to T_{IC} at which the commensurate antiferromagnetic state is reached *via* a first order

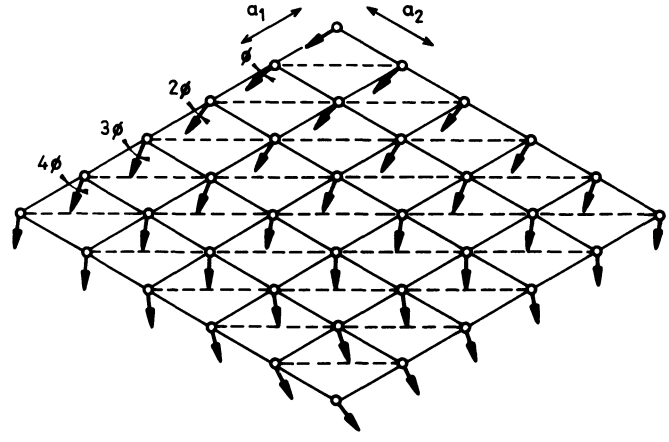

Fig. 1. — Helimagnetic ordering within the basal plane for $NiBr_2$ at $T = 4.2$ K.

transition [6]. It is rather unusual to observe an incommensurate phase at low temperatures and a commensurate one at higher temperatures. This behaviour can be understood if the exchange interactions within (001) planes (J_1, J_2 and J_3) have values such as to be very close to a Lifshitz point [7]. When the helical ordering is the stable state at $T = 0$, Villain has shown [8] that with increasing temperature the magnetic excitations will induce fluctuations between helical states of opposite chirality, thereby driving the system towards a commensurate phase [8], or, in two dimensions, to a chiral disordered phase [9]. In order to understand the magnetic properties of this compound and the mechanism which drives the incommensurate-commensurate phase transition, a precise determination of the exchange and anisotropy parameters is needed. The determination presented in this paper, has been obtained from an investigation of the spin wave dispersion relations in the helimagnetic state at low temperature ($T = 4.2$ K) by inelastic neutron scattering techniques.

2. **Theory.** — In this section we briefly sketch the theoretical framework used for the interpretation of our experimental data on $NiBr_2$. All the following results refer to a three dimensional rhombohedral Bravais lattice, which is the case of $NiBr_2$.

Assuming the z-axis to be perpendicular to the (001) plane the hamiltonian can be written as :

$$H = - \sum_{i,j} J_{ij} \mathbf{S}_i \mathbf{S}_j + D \sum_i (S_i^z)^2 \qquad (1)$$

where $\mathbf{S}_i$ is the spin of the Ni^{2+} ion at site i ($S = 1$) and D is the single-ion anisotropy constant which is positive in the present case of an easy plane anisotropy (XY-system). As regards, the exchange interactions J_{ij}, we will take into account, the first, second and third neighbours in-plane exchange integrals J_1, J_2 and J_3 together with the inter plane exchange integral J' (Fig. 2).

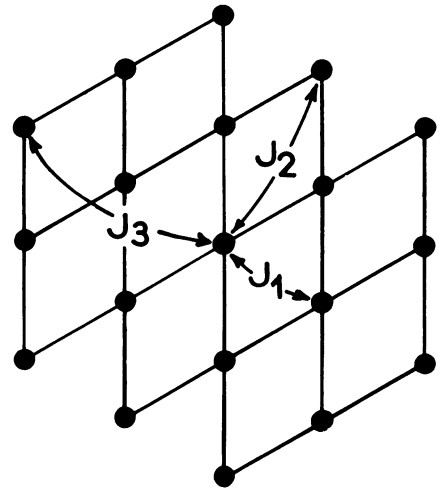

Fig. 2. — Definition of the in-plane exchange integrals.

In the case of a helimagnetic structure described by a wave vector $\mathbf{k}_0 = [k_x, k_y, k_z]$ the classical energy of the spin system can be written as [8, 9] :

$$E(k_x, k_y, k_z) = - J(\mathbf{k})\, S^2$$

where $J(\mathbf{k})$ is the Fourier transform of the exchange integrals.

$$J(\mathbf{k}) = 2J_1[\cos\alpha_x + \cos\alpha_y + \cos(\alpha_x + \alpha_y)] + 2J_2[\cos(2\alpha_x + \alpha_y) + \cos(\alpha_x + 2\alpha_y) + \cos(\alpha_x - \alpha_y)] + 2J_3[\cos 2\alpha_x + \cos 2\alpha_y + \cos 2(\alpha_x + \alpha_y)] + 2J'\left[\cos\left(\frac{2\alpha_x + \alpha_y + \alpha_z}{3}\right) + \cos\left(\frac{-\alpha_x + \alpha_y + \alpha_z}{3}\right) + \cos\left(\frac{\alpha_x + 2\alpha_y - \alpha_z}{3}\right)\right] \qquad (2)$$

where $\alpha_v = 2\pi k_v$ with $v = x, y, z$.

For a given set of the exchange integrals the stable magnetic structures are given by the minima of $E(k_x, k_y, k_z)$ i.e. they are given by the three equations :

$$\frac{\partial E}{\partial k_x} = \frac{\partial E}{\partial k_y} = \frac{\partial E}{\partial k_z} = 0\,. \qquad (3)$$

The corresponding phase diagram has been calculated by Rastelli *et al.* [10] for a rhombohedral lattice when only two exchange integrals are taken into account ($J_3 = 0$) and in the case of a planar hexagonal lattice ($J' = 0$). In the latter case the results, as given in figure 3, indicate that there exist three commensurate phases, with a ferromagnetic ($\mathbf{k} = 0$), an antiferromagnetic ($\mathbf{k} = \langle 1/2, 0 \rangle$) and a triangular ($\mathbf{k} = \langle 1/3, 1/3 \rangle$) structure, as well as two helical phases propagating along a $\langle 1, 0 \rangle$ or a $\langle 1, 1 \rangle$ direction. However, for $NiBr_2$ it is necessary to extent the calculations to non-zero values of J'.

If we consider only the structures associated with the wave vector $\mathbf{k} = \langle \tau, \tau, k_z \rangle$ as actually observed in $NiBr_2$, the possible values of k_z are given by the following equation :

$$\frac{\partial E}{\partial k_z} = J'[2\cos(2\pi\tau) + 1] \sin\left(\frac{2\pi k_z}{3}\right) = 0$$

which has the two solutions $k_z = 0$ and $k_z = 3/2$, corresponding respectively to a ferromagnetic coupling ($J' > 0$) and an antiferromagnetic coupling ($J' < 0$) between adjacent planes.

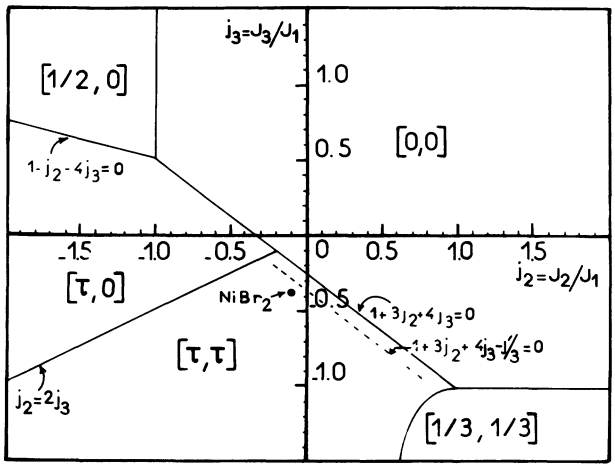

Fig. 3. — Phase diagram for a layered rhombohedral lattice with a planar anisotropy.

The last solution corresponds indeed to the case of $NiBr_2$. The equation $\partial E/\partial\tau = 0$ subsequently gives a relation between J_1, J_2, J_3, J' and τ.

$$J_1 - 3J_2 - J' + 2(J_1 - 2J_3)\cos 2\pi\tau + \\ + 12J_2\cos^2 2\pi\tau + 16J_3\cos^3 2\pi\tau = 0. \quad (4)$$

Within the framework of the molecular field theory, equation (4) predicts the existence of a second order transition between an antiferromagnetic phase ($\mathbf{k} = \langle 003/2 \rangle$) and a helimagnetic phase described by the wave vector $\mathbf{k} = \langle \tau\tau 3/2 \rangle$ if the exchange integrals are allowed to vary.

The bordering line between the two phases is given by :

$$3J_1 + 9J_2 + 12J_3 - J' = 0.$$

In figure 3 one can see that the main influence of introducing a finite $J' < 0$ is to shift this line in order to increase the stability range of the antiferromagnetic phase ($\mathbf{k} = \langle 003/2 \rangle$).

It must be emphasized that the observed commensurate-incommensurate transition in $NiBr_2$ is in fact of first order. It has been proposed that this transition might result from large fluctuations, which would give rise to a renormalization of the exchange integrals and thus to a crossing of the bordering line [6].

The spin wave spectrum can be easily obtained from the hamiltonian (1) using the standard Holstein-Primakoff transformation to boson operators. Taking into account only the lowest order terms a quadratic hamiltonian is obtained which is readily diagonalized [11]. However the $(S_i^z)^2$ term must be treated very carefully [12] due to the finite value of the spin, indeed D must be changed in $\tilde{D} = D\left(1 - \frac{1}{2S}\right)$.

In case of a magnetic order described by a wave vector $\mathbf{k}_0$ the energy of the spin wave excitation with wave vector $\mathbf{q}$ is given by :

$$\omega(\mathbf{q}) = 2S\left[J(\mathbf{k}_0) - \frac{J(\mathbf{q}+\mathbf{k}_0) + J(\mathbf{q}-\mathbf{k}_0)}{2}\right]^{1/2}\left[J(\mathbf{k}_0) - J(\mathbf{q}) + \tilde{D}\right]^{1/2} \quad (5)$$

where $J(\mathbf{q})$ is defined as :

$$J(\mathbf{q}) = \sum_{(\mathbf{R}_i - \mathbf{R}_j)} J_{ij}\, e^{-2\pi i\mathbf{q}(\mathbf{R}_i - \mathbf{R}_j)}.$$

This dispersion relation, equivalent to that given by Rastelli *et al.* [10], is defined within the whole Brillouin zone of the rhombohedral lattice.

From (2) and (5) we can obtain the energy of the magnons which propagate along the **c**-axis ($\mathbf{q} = [0, 0, q_c]$).

$$\omega(0, 0, q_c) = 2S\left[2|J'|(2\cos 2\pi\tau + 1)\left(1 - \cos\frac{2\pi q_c}{3}\right)\right]^{1/2}\left[2|J'|(2\cos 2\pi\tau + 1 + 3\cos\frac{2\pi q_c}{3}) + \tilde{D}\right]^{1/2}.$$

Since τ and $\tilde{D}$ are small-valued we may write :

$$\omega(0, 0, 3/2) \simeq \sqrt{48\,\tilde{D}\,|J'|\,S} \quad (6)$$
$$\omega(0, 0, 3/4) \simeq 12J'S.$$

Equations (6) allow us to determine D and J' by measuring the energy gap in the spin wave spectrum at the zone boundary ($q_c = 3/2$) and at the middle of the zone ($q_c = 3/4$).

3. **Experimental.** — $NiBr_2$ crystallizes in the $CdCl_2$ structure which has the rhombohedral space group $R\bar{3}m$. The nickel ions are on a single Bravais lattice. In the equivalent hexagonal system, the cell parameters are $a = 3.65$ Å and $c = 18.23$ Å. The reciprocal lattice and the first Brillouin zone of $NiBr_2$ are given in figure 4. A single crystal of about 1 cm^3 was prepared according to the method described in reference [6].

Inelastic neutron scattering experiments have been performed using the triple axis spectrometer DN_1

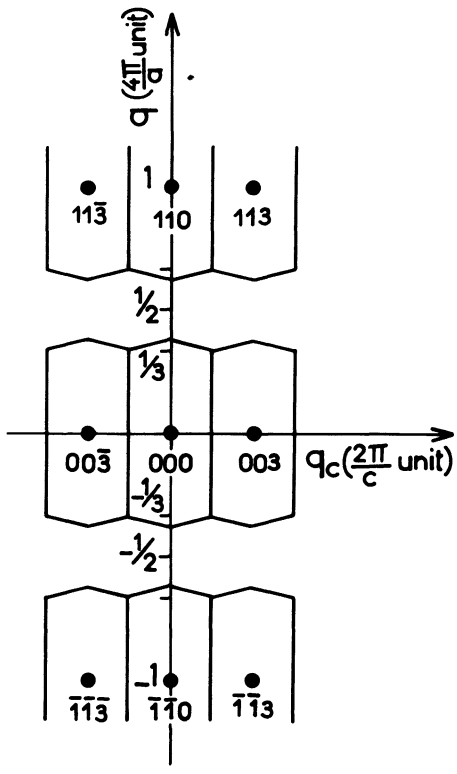

Fig. 4. — Reciprocal lattice of $NiBr_2$.

at the reactor Siloe of the C.E.N.-Grenoble. Incident neutrons of 1.2 Å and 2.2 Å, obtained from copper and graphite monochromators, were used to measure both the high and the low energy excitations. Pyrolytic graphite with (002) planes was used for the energy analysis. The collimation on both sides of the sample was about 30'.

The crystal was oriented with the [110] and [001] reciprocal directions in the equatorial plane. The excitation energy of the spin waves were measured at $T = 4.2$ K along the [110] direction in the [003] and [006] Brillouin zones in the helimagnetic state.

4. **Results and analysis.** — The excitation energies less than 7 meV were measured with neutrons of incident energy 16 meV ($\lambda = 2.2$ Å). For the energy transfers larger than 10 meV an incident energy of 56 meV ($\lambda = 1.2$ Å) has been used. For these two wave lengths the instrumental resolution in energy and q-space has been determined and the results are given in table I. They correspond to standard conditions.

The energies of the magnetic excitations for wave vectors along [110] have been studied for different values of q_c ($q_c = 0$, 0.75 and 1.5). Typical scans in energy or in q-space are shown in figures 5, 6 and 7. q-scans give a q-width of about 0.08 r.l.u. which is much larger than the q-resolution (0.03 r.l.u.) as can

Table I. — *Energy and q-width of the resolution function (calculated from the experimental collimations).*

λ (Å)	E_i (meV)	ΔE (meV)	Δq (r.l.u.)
1.2	56	5.0	0.050
2.2	16	1.3	0.030

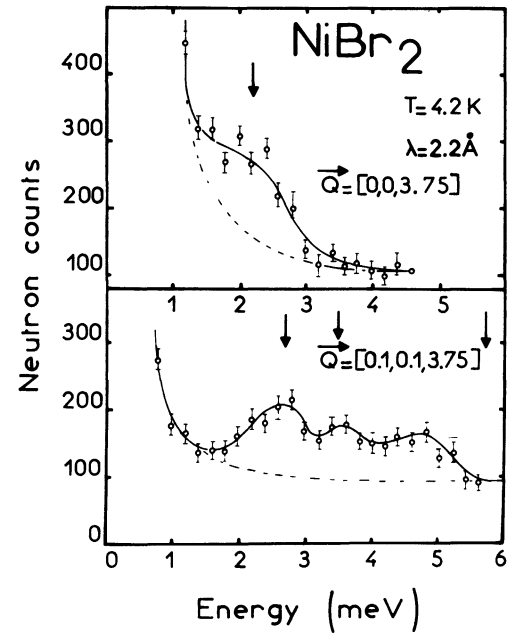

Fig. 5. — Energy scans performed at $T = 4.2$ K in the [003] Brillouin zone. For $\mathbf{q} = [0, 0, 0.75]$ only the IPC can be observed and they give a single peak for this special q-point. For $\mathbf{q} = [0.1, 0.1, 0.75]$ both the OPC and the IPC are measured.

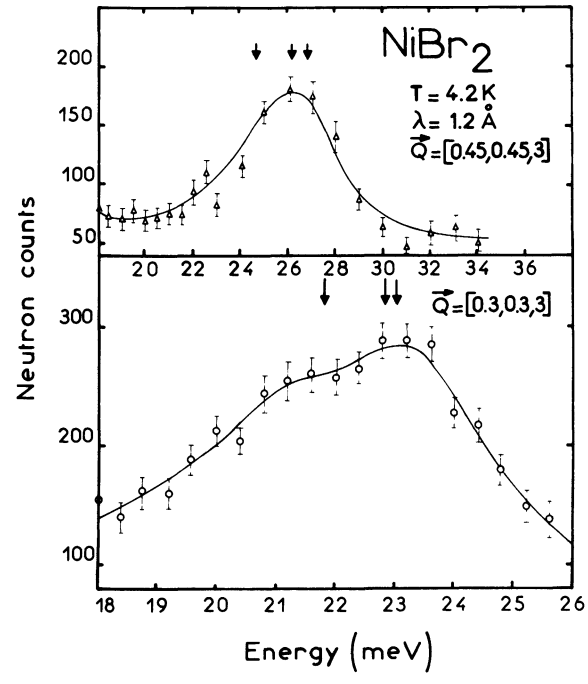

Fig. 6. — Energy scans performed at $T = 4.2$ K in the [003] Brillouin zone giving the high energy part of the dispersion curve. At $\lambda = 1.2$ Å the resolution is not good enough to separate the OPC and the IPC peaks. Moreover the curvature of the dispersion curve is clearly seen for the wave vector $\mathbf{q} = [0.3, 0.3, 0]$.

be seen in figure 7. This result is not surprising since we will see below that it is due to the helimagnetic nature of the magnetic ordering.

For a planar helimagnetic order with one Bravais lattice, the inelastic scattering cross section is given by [13] :

$$\frac{d^2\sigma(\mathbf{Q},\omega)}{d\Omega\, d\omega} \sim \left(1 - \frac{Q_z^2}{Q^2}\right) \exp(\phi_q) \left[(\langle \eta_q \rangle + 1)\, \delta(\omega - \omega_q) + \langle \eta_q \rangle\, \delta(\omega + \omega_q)\right] +$$

$$+ \frac{1}{4}\left(1 + \frac{Q_z^2}{Q^2}\right) \{ \exp(-\phi_{q+k_0}) \left[(\langle \eta_{q+k_0} \rangle + 1)\, \delta(\omega - \omega_{q+k_0}) + \langle \eta_{q+k_0} \rangle\, \delta(\omega + \omega_{q+k_0})\right]$$

$$+ \exp(-\phi_{q-k_0}) \left[(\langle \eta_{q-k_0} \rangle + 1)\, \delta(\omega - \omega_{q-k_0}) + \langle \eta_{q-k_0} \rangle\, \delta(\omega + \omega_{q-k_0})\right] \} \qquad (7)$$

where

$$\phi_q = \tanh^{-1}\left(\frac{J(\mathbf{q}) - \dfrac{J(\mathbf{q}+\mathbf{k}_0) + J(\mathbf{q}-\mathbf{k}_0)}{2} - \tilde{D}}{2J(\mathbf{k}_0) - J(\mathbf{q}) - \dfrac{J(\mathbf{q}+\mathbf{k}_0) + J(\mathbf{q}-\mathbf{k}_0)}{2} + \tilde{D}}\right),$$

$$\langle \eta_q \rangle = \frac{1}{\exp\left(\dfrac{\hbar\omega_q}{kT}\right) - 1} \quad \text{is the Bose factor.}$$

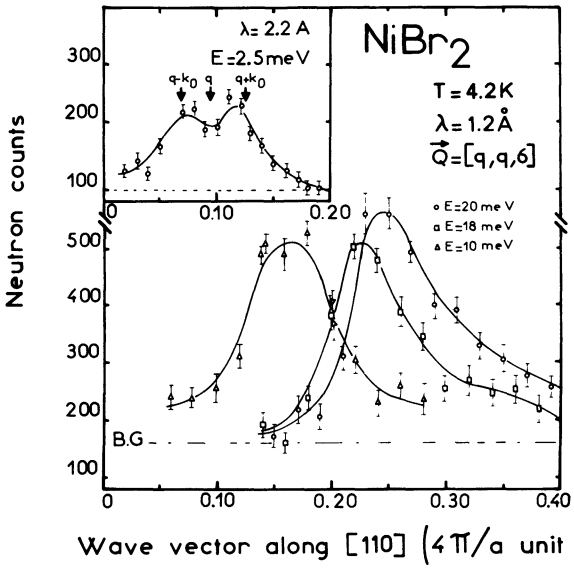

Fig. 7. — Q-scans performed at $T = 4.2$ K in the [006] Brillouin zone.

The scattering vector is equal to $\mathbf{Q} = \mathbf{q} + \mathbf{H}$ where $\mathbf{H}$ is a reciprocal lattice vector and the wave vector $\mathbf{q}$ of the excitation is restricted to the first Brillouin zone.

Physically the first term of equation (7) arises from the fluctuations of the moment component perpendicular to the easy plane, whereas the remaining two terms arise from the fluctuations of the moment components within the easy plane. The fluctuations of the out-of-plane component (OPC) are due to spin waves with an energy $\omega(\mathbf{q})$ and then they allow a direct determination of the dispersion relation. For the fluctuations of the in-plane components (IPC) the situation for the helimagnet is more complex than for an antiferromagnet for which $\mathbf{k}_0 = \mathbf{H}/2$. Since, in the case of a helimagnetic order, the magnetic moments rotate within the basal plane, it is necessary to define a local quantization axis which also rotates with the angle $2\pi\mathbf{k}_0\,\mathbf{R}_n$. Therefore, at a wave vector $\mathbf{q}$ the IPC fluctuations give rise to two additional neutron peaks at energy transfer $\omega(\mathbf{q} + \mathbf{k}_0)$ and $\omega(\mathbf{q} - \mathbf{k}_0)$.

The situation described above concerns a single domain structure of wave vector $\mathbf{k}_1 = \mathbf{k}_0$ (domain K_1). In fact, below T_{IC}, a triple domain structure is formed with wave vectors $\mathbf{k}_2$ and $\mathbf{k}_3$, which are deduced from $\mathbf{k}_0$ by $\pm\, 2\pi/3$ rotations (domains K_2 and K_3). One can easily show that along the measured direction, the spin wave spectrum, for a given $\mathbf{q}$, consists of five peaks, corresponding to ω_q, $\omega_{q\pm k_1}$ and $\omega_{q\pm k_{2,3}}$. Computer simulations show that $\omega_{q-k_1} \simeq \omega_{q-k_{2,3}}$ and $\omega_{q+k_1} \simeq \omega_{q+k_{2,3}}$, so that only three peaks are effectively observable, taking into account the $\mathbf{q}$ and energy resolution, and the effect of the domains can be neglected in the present case.

Therefore in a helimagnet for a given domain an energy-scan will in general show three peaks, at energies $\omega(\mathbf{q})$, $\omega(\mathbf{q} + \mathbf{k}_0)$ and $\omega(\mathbf{q} - \mathbf{k}_0)$, whereas for an antiferromagnet $+\,\mathbf{k}_0$ and $-\,\mathbf{k}_0$ are equivalent so that only two peaks will be observed. Since both types of fluctuations are due to spin waves there is in fact only a single dispersion relation $\omega(\mathbf{q})$, however in a neutron scattering experiment the OPC and the IPC contributions are seen differently. The OPC and the IPC dispersion relations are thus the same, except that the latter are deduced from the former by a translation of $\pm\,\mathbf{k}_0$ in the (ω, q) space. To obtain the true dispersion relation, the practical problem to be solved is therefore to deduce the OPC and the IPC contribution separately from the data. This can be done by

changing the orientation of the scattering vector with respect to the c-axis and by calculating the inelastic cross section given by equation (7). The dispersion relation $\omega(\mathbf{q})$ associated with the OPC is linear for small q values and passes through the origin in agreement with the Goldstone theorem, whereas the IPC gives rise to two dispersion relations both merging from the point $\mathbf{q} = \mathbf{k}_0$.

In the present case of $NiBr_2$, for e.g. a wave vector $\mathbf{q} = [q, q, 0]$, the OPC will give a peak at $\omega(q, q, 0)$ and the IPC will give two peaks at $\omega(q + \tau, q + \tau, 3/2)$ and $\omega(q - \tau, q - \tau, 3/2)$. These three peaks will indeed be very close in energy because the anisotropy of Ni^{2+} is small and the incommensurate component of the wave vector describing the structure is also small ($\tau = 0.027$ at $T = 4.2$ K [6]).

For a wave length $\lambda = 1.2$ Å the instrumental widths in q and ω were such that it was not possible to separate the three contributions at $\omega(\mathbf{q})$, $\omega(\mathbf{q} + \mathbf{k}_0)$ and $\omega(\mathbf{q} - \mathbf{k}_0)$, which are of the same order of magnitude for $q > 0.2$ (r.l.u.). Accordingly a single broadened peak was observed (Figs. 6 and 7). With a wave length $\lambda = 2.2$ Å, for which the instrumental resolution in q and ω is much improved, it has been possible to separate these different contributions. This can be seen in figures 5 and 7 where we observe two peaks at $\omega(\mathbf{q} \pm \mathbf{k}_0)$ or three peaks at $\omega(\mathbf{q}), \omega(\mathbf{q} \pm \mathbf{k}_0)$ depending on the value of the ratio Q_z/Q.

From the above discussion, it is clear that an experimental determination of the dispersion curve is indeed much more difficult for a helimagnetic system such as $NiBr_2$ than for a ferro- or an antiferromagnetic structure and a great care must be taken in the analysis.

Figures 6 and 7 show asymmetric line shapes in the ω or q-scan profiles for a wave vector $\mathbf{q} = [0.25, 0.25, 0]$ and an energy of about 20 meV. As we shall see later this can be explained in terms of a resolution effect when the curvature of the spin wave dispersion curve is taken into account. Nevertheless the position of the maximum of the peak is weakly affected by this effect.

The dispersion curves obtained along the $[qq0]$ direction for $q_c = 0$, 0.75 and 1.5 are collected in figure 8. For small q values it has not been possible to measure the spin wave energies for $q_c = 0$ and $q_c = 1.5$ because the energy resolution was not sufficient. Consequently, the gap at $\mathbf{q} = [0, 0, 1.5]$, which from equation (6) would yield the anisotropy parameter D, has not been determined.

Figure 8 shows that for $q > 0.15$ the dispersion of the spin waves is practically independent of q_c, indicating that J' must be relatively small. Indeed, J' can be derived directly from the gap at $\mathbf{q} = [0, 0, 0.75]$. An energy scan at $\mathbf{q} = [0, 0, 0.75]$ (Fig. 3) gives the value $\hbar\omega\ (0, 0, 0.75) = (2.2 \pm 0.1)$ meV and from equation (6) we get :

$$J' = -(0.182 \pm 0.005)\ \text{meV}.$$

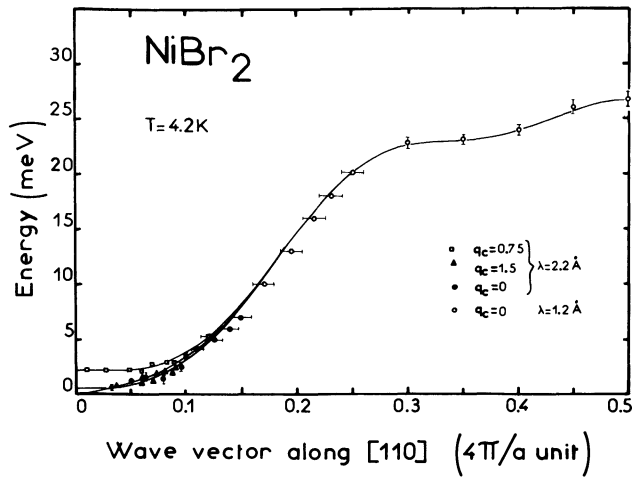

Fig. 8. — Dispersion relations of spin waves propagation along $[q, q, q_c]$ directions in the helimagnetic state of $NiBr_2$ at $T = 4.2$ K.

Computer simulations show that for $q > 0.3$ the spin wave dispersion will indeed depend only on the in-plane exchange integrals J_1, J_2 and J_3. In fact there are only two independent parameters here because equation (4) relates J_2 to J_1, J_3 and J'. As J' is known, J_1 and J_3 are unequivocally determined by fitting the part of the dispersion curve for $0.3 \leqslant q \leqslant 0.5$. The best fit was obtained for the following combination :

$$J_1 = (1.56 \pm 0.02)\ \text{meV}$$

$$J_3 = -(0.41 \pm 0.02)\ \text{meV}$$

which gives from equation (4) :

$$J_2 = -(0.018 \pm 0.02)\ \text{meV}.$$

The anisotropy constant D has been estimated by fitting the low-q region of the dispersion curve for $q_c = 0$, 0.75 and 1.5. We obtain the value :

$$D = (0.08 \pm 0.05)\ \text{meV}.$$

Clearly high resolution experiments at low q values would be needed to get a more accurate value.

The calculated spin wave dispersion curves, using the values of the parameters J_1, J_2, J_3, J' and D determined above, are shown in figure 8 by the full lines. The agreement with the experiment is quite good.

5. **Discussion.** — The ratio of inter to intra planar exchange constants is found to be $-J'/J_1 = 0.117$ for $NiBr_2$, which is three times larger than for $NiCl_2$ [14] ($-J'/J_1 = 0.035$), but smaller than for $CoBr_2$ [15] ($-J'/J_1 = 0.483$).

As for $NiCl_2$ [14], the nearest neighbour exchange interaction within the plane J_1 has the strongest value and is ferromagnetic, but for $NiBr_2$ the exchange interaction J_3 must be taken into account and has a

relatively important value ($-J_3/J_1 = 0.262$). A similar result has been found in $CoBr_2$ [15] ($-J_3/J_1 = 0.168$). Therefore it will be useful to measure the dispersion curve along a [q, q, 0] direction for $NiCl_2$ to check if the exchange constant J_3 is indeed negligible as it was assumed in [14].

The values of the exchange integrals J_1, J_2, J_3 and J' and of the anisotropy parameter D determined from the spin wave dispersion relations can be used to compare the results obtained by other experimental techniques, e.g. magnetization, susceptibility, or antiferromagnetic resonance measurements.

Antiferromagnetic resonance experiments give resonance lines at the frequencies ν_1 ($H=0$) = (6 ± 1) GHz [3] when the magnetic field is applied within the (001) plane and ν_2 ($H = 0$) = (204 ± 2) GHz [16, 17] when the magnetic field is applied perpendicular to the (001) plane. These resonance lines have been observed in the antiferromagnetic phase. The frequency ν_1 corresponds to the energy gap at $\mathbf{q} = 0$ which is due to the very weak in-plane anisotropy, which has not been taken into account in our calculations. The frequency ν_2 is associated with the planar anisotropy which gives an energy gap for the wave vector $\mathbf{q} = [003/2] : h\nu_2 (H = 0) = \hbar\omega(0, 0, 3/2)$.

The AFMR experiments [16, 17] give a value $h\nu_2$ ($H = 0$) = (0.84 ± 0.01) meV. From this AFMR value a more accurate determination of the planar anisotropy parameter can be obtained, namely :

$$D = (0.15 \pm 0.01)\ \text{meV}$$

which is about two times larger than the value obtained from the spin wave spectrum.

We remark that this change in the value of the D parameter does not affect the determination of the exchange integrals in the above. It must be emphasized that the planar anisotropy is about four times larger in $NiBr_2$ than in $NiCl_2$ and this strongly affects the dispersion relation in the low-q region. The larger D value could be explained by the more important distortion of the bromide octahedra in $NiBr_2$, as can be seen by comparing the c/a ratio for $NiBr_2$ (4.99) with that for $NiCl_2$ (4.96).

The (H, T) magnetic phase diagram of $NiBr_2$ has been deduced from high-field magnetization experiments [18].

A magnetic field applied within the basal plane is found to induce a spinflop transition at the critical field H_c between the helimagnetic phase and an antiferromagnetic flopped phase. In the latter the antiferromagnetic direction is perpendicular to the magnetic field for $H \gtrsim H_c$ and with increasing field each sublattice is rotated towards the field direction to reach the saturated paramagnetic state. At $T = 4.2$ K (Fig. 9) the critical field is found to have the value $H_c = 27$ kOe whereas the magnetization is found to saturate in very high fields, namely at $H_s = 380$ kOe, for a saturation value of $\sigma_s = g_\perp \mu_B S = 2.27\ \mu_B$.

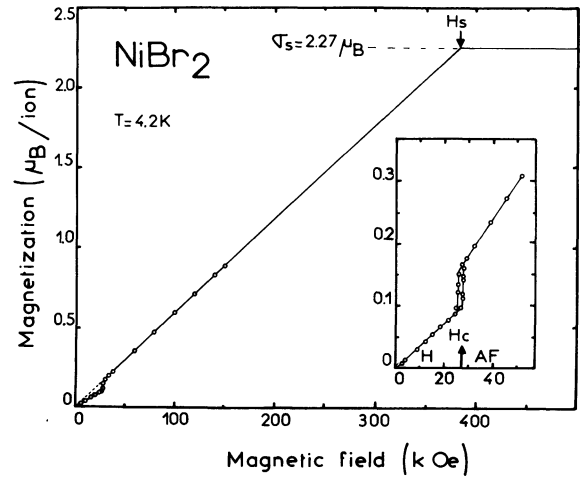

Fig. 9. — High field magnetization of $NiBr_2$ for a magnetic field applied within the basal plane. Both results of static [19] and pulsed field [18] measurements have been reported. The insert shows clearly the first order transition between the helimagnetic and the antiferromagnetic phases and the susceptibility discontinuity associated with this transition.

This saturation field depends indeed only on the interplane exchange constant J' :

$$H_s = \frac{24 \mid J' \mid S^2}{g_\perp \mu_B S}$$

The value $J' = -0.182$ meV gives a saturation field $H_s = (380 \pm 10)$ kOe in excellent agreement with the experimental value.

On the other hand, both the inter plane and the intra plane exchange constants are involved in the critical field H_c which is defined by :

$$E_H - \tfrac{1}{2}\chi_H H_c^2 = E_{AF} - \tfrac{1}{2}\chi_{AF} H_c^2$$

where E_H, χ_H, E_{AF} and χ_{AF} are the energy and the susceptibility of the helimagnetic and the antiferromagnetic structure. Then the critical field is given by :

$$H_c = H_s \sqrt{\frac{E_{AF} - E_H}{12 \mid J' \mid S^2 (1 - \chi_H/\chi_{AF})}}.$$

Using the exchange constants determined above we evaluate from equation (2) $E_{AF} - E_H \simeq 0.007$ meV. This value together with the experimental ratio $\chi_H/\chi_{AF} = 0.58$ [19] (Fig. 9) lead to a critical field value $H_c = 33$ kOe which is very close to the experimental one (27 kOe). These good agreements give us confidence in the determination of the exchange constants J_1, J_2, J_3 and J'.

It has been shown [19] that a hydrostatic pressure reduces the stability range of the helimagnetic phase which is suppressed by a pressure of 10.6 kbar. The pressure reduces the susceptibility of the antiferromagnetic phase χ_{AF}, whereas that of the helimagnetic state is unchanged. Therefore the main effect of pres-

sure is to increase the value of the inter plane interaction J' and consequently the helimagnetic structure is destabilized (see equation (4)). May be a similar behaviour can be invoked to explain the incommensurate-commensurate phase transition which occurs in zero field.

Finally the values of the exchange interactions can be used to calculate the paramagnetic Curie temperature θ_p which is given by :

$$k\theta_p = \tfrac{2}{3} S(S + 1)[6 J_1 + 6 J_2 + 6 J_3 + 6 J'].$$

We get a value $\theta_p = 76$ K which is much larger than the experimental one $\theta_p \simeq 38$ K as determined from susceptibility measurements performed below room temperature [18]. The difference can be ascribed to short-range order effects. Clearly, measurements must be done in a much higher temperature range in order to get a reliable value for θ_p.

Acknowledgments. — We would like to thank Dr. E. Rastelli for fruitful discussions and Dr. L. J. de Jongh for a critical reading of the manuscript.

References

[1] DAY, P., DINSDALE, A., KRAUSZ, E. R. and ROBBINS, D. J., *J. Phys. C* **9** (1976) 2481.

[2] BILLEREY, D., TERRIER, C., MAINARD, D. and MERIEL, P., *C. R. Hebd. Séan. Acad. Sci.*, Serie B **284** (1977) 495.

[3] KATSUMATA, K. and DATE, M., *J. Phys. Soc. Japan* **27** (1969) 1360.

[4] MORITO, Y. and DATE, M., *J. Phys. Soc. Japan* **29** (1970) 1090.

[5] DAY, P. and ZIEBECK, K. R. A., *J. Phys. C* **13** (1980) L 01.

[6] ADAM, A., BILLEREY, D., TERRIER, C., MAINARD, R., REGNAULT, L. P., ROSSAT-MIGNOD, J. and MERIEL, P., *Solid State Commun.* **35** (1980) 1.

[7] HORNREICH, R. M., LUBAN, M. and SHTRIKMANN, S., *Phys. Rev. Lett.* **35** (1975) 1678.

[8] LUTTINGER, J. M. and TISZA, L., *Phys. Rev.* **70** (1946) 954.

[9] VILLAIN, J., *J. Phys. Chem. Solids* **11** (1959) 303.
BERTAUT, E. F., in *Magnetism*, edited by Rado and Suhl (1963) Tome III.

[10] RASTELLI, E., TASSI, A. and REATTO, L., *Physica* B + C **97 B** (1979) 1.

[11] WALKER, L. R., in *Magnetism*, edited by Rado and Suhl (1963) Tome I.

[12] LINDGARD, P. A. and KOWALSKA, A., *J. Phys. C* **9** (1976) 2081.

[13] LINDGARD, P. A., KOWALSKA, A. and LAUT, P., *J. Phys. Chem. Solids* **28** (1967) 1357.

[14] LINDGARD, P. A., BIRGENEAU, R. J., ALS-NIELSEN, J. and GUGGENHEIM, H. J., *J. Phys. C* **8** (1975) 1059.

[15] YOSHIZAWA, H., UBUKOSHI, K. and HIRAKAWA, K., *J. Phys. Soc. Japan* **48** (1980) 42.

[16] ADAM, A., BILLEREY, D., TERRIER, C., KATSUMATA, K., MAGARIÑO, J., TUCHENDLER, J., *Phys. Lett.* **79A** (1980) 353.

[17] TUCHENDLER, J., KATSUMATA, K., BILLEREY, D., ADAM, A., TERRIER, C., to be published.

[18] ADAM, A., BILLEREY, D., TERRIER, C., to be published.

[19] ADAM, A., BILLEREY, D., TERRIER, C., BARTHOLIN, H., REGNAULT, L. P., ROSSAT-MIGNOD, J., *Phys. Lett.* **84A** (1981) 24.